# Brillouin light scattering investigation of magnetostatic modes in symmetric and asymmetric NiFe/Cu/NiFe trilayered wires

G. Gubbiotti
*INFM CRS–SOFT, c/o Università di Roma "La Sapienza", I–00185 Rome, Italy and*
*INFM UdR–Perugia, c/o Dipartimento di Fisica, Università di Perugia, Via A. Pascoli, 06123 Perugia, Italy*

M. Kostylev[1] and N. Sergeeva[1,2]
[1]*St. Petersburg Electrotechnical University, 197376, St. Petersburg, Russia*
[2]*LPMTM, Institut Galilée, Université Paris 13, 99 Avenue J.-B. Clément, 93430 Villetaneuse, France*

M. Conti
*Istituto Nazionale Fisica della Materia, Dipartimento di Fisica, Università degli Studi di Perugia, Via A. Pascoli, 06123 Perugia, Italy*

G. Carlotti
*INFM–National Center for nanoStructures and bioSystem at Surfaces (S3), Dipartimento di Fisica, Università di Perugia, Via A. Pascoli, 06123 Perugia, Italy*

T. Ono
*Institute for Chemical Research, Kyoto University, Uji, Kyoto 611-0011, Japan*

A. N. Slavin
*Department of Physics, Oakland University, Rochester, Michigan 48309, USA*

A. Stashkevich
*LPMTM, Institut Galilée, Université Paris 13, 99 Avenue J.-B. Clément, 93430 Villetaneuse, France*
(Received 2 July 2004; published 17 December 2004)

The peculiarities of magnetostatic resonances of trilayered wires (700 nm wide) consisting of two ferromagnetic permalloy layers, coupled by dipolar interaction across a nonmagnetic Cu spacer, have been comprehensively studied both experimentally and theoretically. Both a symmetric structure, NiFe(30 nm)/Cu(10 nm)/NiFe(30 nm), and an asymmetric one, NiFe(10 nm)/Cu(10 nm)/NiFe(30 nm), were analyzed. Brillouin light scattering (BLS) from thermally excited spin waves, has been performed as a function of the incidence angle of light and of the intensity of the external applied field. A number of discrete peaks, corresponding to the resonant frequencies of the trilayered structures have been observed in BLS spectra. To achieve a satisfactory interpretation of the experimental results, substantial improvements of previous theoretical models were necessary. In this case, in fact, due to the rather large value of the ferromagnetic layers thickness, the dipole interaction between magnetic layers associated with the nondiagonal terms of the tensorial Green's functions (describing a dynamic dipolar magnetic field induced by one magnetic layer in the other one) gives significant contributions to the resonant frequencies.

DOI: 10.1103/PhysRevB.70.224422 PACS number(s): 75.70.Cn, 78.35.+c, 75.30.Ds

## I. INTRODUCTION

A detailed comprehension of the dynamic behavior of nanopatterned magnetic structures is of great importance from the theoretical point of view, given the new features introduced by the reduced dimensionality. The applied aspect of these studies should not be underestimated, either. A rapid increase of processor speeds in modern computers has lead to the necessity of writing gigabits of information in a fraction of a second. With the advance of shorter and shorter time scales, the fundamental dynamic processes demand for a deep physical understanding, in particular to make use of them for magnetic recording media. Central problems are the inevitable generation of spin waves in a magnetic system excited at gigahertz rates and the high-frequency thermal fluctuation of the magnetization (magnetic noise) in giant magnetoresistive heads which provide a fundamental limitation of the ability to scale down the device size and increase the operating frequency.[1]

If magnetic nanoelements are brought too close to one another, spurious collective magnetostatic modes will be excited through increased "horizontal" coupling. In the case of nanodots, where the fundamental magnetic state corresponds to a vortex configuration, this leads to a considerable mutual influence between the dots during the magnetization reversal,[2] as well as to a magnetostatic coupling[3] between the dynamic modes of individual vortices.[4] Similarly, in the case of nanowires of cylindrical cross section, both in the theory[5] and in the experiment,[6] collective modes, due to the interplay between individual wires, were reported.

 

Until lately, the problem of localization of a spin wave mode on an isolated one dimensional object, such as a monolayer stripe, had no solution except purely numerical.[7] It was generally accepted that the dynamic magnetic field at the edges of the film tends to zero or, in other words, the spins at the edges of the film are totally "pinned."[8] An analytical formalism which allowed estimating the profiles of the dynamic magnetization across an individual mono-layer ferromagnetic stripe was proposed in Ref. 9. Special attention has been paid to the behavior of the magnetization at the stripe edges. Thus the fruitful concept of "effective dipolar pinning" has been introduced and the exact quantization conditions formulated. This approach proved to be effective and in more recent papers it has been extended to collective modes on an array of monolayer stripes[10] and individual resonances on an isolated bilayer stripe.[11] In the latter case, some of the theoretical predictions have been verified experimentally.[12]

On the other hand, the "vertical" coupling between individual layers in a ferromagnetic multilayer also plays a very important role in the frequency response of nanoelements. The switching speed of layered magnetic devices has been of interest since the application of magnetic core memories. Recently, experimental measurements as well as numerical micromagnetic simulations were applied to analyze the thermal magnetization noise,[13] the reversal modes, and the switching times of MRAM memory cells.[14]

The purpose of this paper is a comprehensive investigation of magnetostatic modes in arrays of trilayered magnetic wires in which two ferromagnetic layers, separated by a nonmagnetic spacer, are coupled by dipolar interaction, only. The present study embraces the case of both symmetrical and nonsymmetrical structures and the influence of a thick spacer on the behavior of magnetic excitations. Brillouin light scattering study of thermally excited spin waves has been performed as a function of the incidence angle of light and of the intensity of the external applied field to resolve individual resonances for the "optical" mode.

A detailed description of the distribution of the dynamic magnetization across the wires width is presented with particular emphasis on the pinning effect. Application of thick structures in the experiment required appropriate improvements to the theoretical description, with respect to the previous approach.[11]

## II. EXPERIMENT

Permalloy ($Ni_{81}Fe_{19}$) wires having width $w=0.7$ $\mu$m and spacing of 0.4 $\mu$m were prepared on thermally oxidized Si substrates by means of e-beam lithography, electron-gun deposition, and lift-off process. Two different arrays have been fabricated: the wires have a trilayered structure NiFe(30 nm)/Cu(10 nm)/NiFe(30 nm) (symmetric structure) and NiFe(10 nm)/Cu(10 nm)/NiFe(30 nm) (asymmetric structure). The wires were arranged in arrays of dimensions of $800\times800$ $\mu m^2$. Figure 1 reports an atomic force microscopy (AFM) image of the symmetric NiFe(30 nm)/Cu(10 nm)/NiFe(30 nm) array of trilayered wires and the layering scheme of the trilayered wires. Part of the magnetic film was left unpatterned to compare the consequences of patterning as measured by BLS.

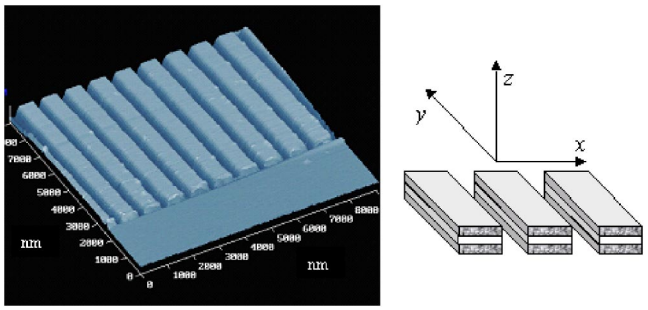


FIG. 1. Atomic force micrograph for the symmetric NiFe(30 nm)/Cu(10 nm)/NiFe(30 nm) trilayered wires. The layering scheme of the wires is also shown together with the system of references axis.

The Brillouin light scattering (BLS) experiments were carried out at the GHOST laboratory, Perugia University,[15] using a Sandercock (3+3)-pass tandem Fabry-Perot interferometer.[16] A beam of about 200 mW of *P*-polarized light from a single-mode solid state laser operating at $\lambda=532$ nm was focused on the sample surface using a camera objective of numerical aperture 2 and focal length 50 mm and the scattered light was collected by the same objective used for focusing the laser beam (backscattering configuration). Since the light scattered from spin waves has a polarization rotated by 90° with respect to the incident one, an analyzer set at extinction (with respect to the polarization of the laser) suppressed the signal from elastically-scattered and surface phonons-scattered light. A dc magnetic field, variable between 0 and 1.0 kOe, was applied along the sample plane, parallel to the wires length (*y*-direction), and perpendicular to the scattering plane (*x*-*z* plane). The sample was mounted on a goniometer to allow rotation around the field direction, i.e. to vary the incidence angle of light, $\theta$, between 6° and 70°. The probed spin-wave wave vector is parallel to the wires width (*x-direction*) and its amplitude, ranging from $0.41\cdot10^5$ $cm^{-1}$ to $2.2\cdot10^5$ $cm^{-1}$, is related to the angle of incidence $\theta$ by $K=(4\pi/\lambda)\sin\theta$. The experimental geometry, showing the orientation of the applied field *H* and the direction of the wave vector *K* with respect to the trilayered wires, is shown in the insets of Figs. 2 and 6.

## III. THEORY

Theoretical calculations presented here are an extension of the method described in Ref. 11 which was developed for the analysis of magnetic excitations in relatively thin structures $KL\ll1$ in which case it proved very effective. Here *L* is the overall thickness of the magnetic structure. The numerical estimations in Ref. 11 have shown that it is still applicable for $KL\approx0.4$. The experiment in Ref. 12 on a thin layered structure proved the adequacy of the theoretical technique. However, in the case considered in this paper, for high values of angles of incidence *KL* can exceed unity and the following improvements were necessary.

We are considering here a magnetic trilayer comprised of two identical films: the upper one (with thickness $L_1$)

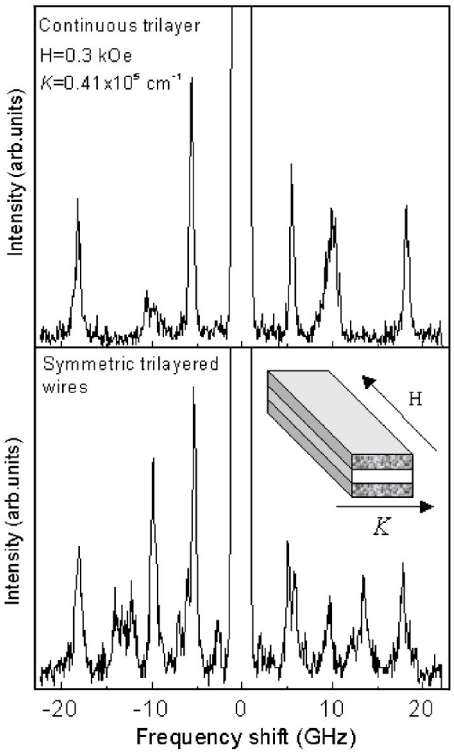


FIG. 2. BLS spectra for the symmetric NiFe(30 nm)/Cu(10 nm)/NiFe(30 nm) structure: (upper panel) unpatterned trilayer and (lower panel) patterned trilayered wires. The spectra are taken in the same experimental conditions: incidence angle of light $\theta=10°$ ($K=0.41\times10^5$ cm$^{-1}$) and external magnetic field of 0.3 kOe, sufficient to ensure sample saturation. The direction of the applied magnetic field and the transferred wavevector with respect to the wires is shown in the inset.

and the lower one (with thickness $L_2$) separated by a nonmagnetic spacer (with thickness $d$), as shown in Fig. 1. Assuming the structure to be magnetized along the $y$ axis, the dynamic magnetizations of the two magnetic films are coupled either via identical components or via different components of tensorial Green's functions $\hat{G}^{(21)}(x,x')$ and $\hat{G}^{(12)}\times(x,x')$. The first kind of coupling is described by $g_{xx}^{(12)}\times(x,x')$, $g_{zz}^{(12)}(x,x')$, $g_{xx}^{(21)}$, $g_{zz}^{(21)}$, while the second one by $g_{xz}^{(12)}(x,x')$, $g_{zx}^{(12)}(x,x')$, $g_{xz}^{(21)}$, $g_{zx}^{(21)}$ [see Eq. 5 in Ref. 11]. In the numerical simulations reported in Ref. 11 only the coupling through the first set of coefficients was taken into account, which is justified for thin magnetic structures. In the results presented below a more rigorous technique, taking into account the second set of coefficients, has been used.

The explicit expressions for the elements $g_{xz}^{(12)}(x,x')$, $g_{zx}^{(12)}(x,x')$, $g_{xz}^{(21)}$, $g_{zx}^{(21)}$ are, as follows:

$$
\begin{aligned}
L_1 g_{Xz}^{(12)}(x,x') &= -L_1 g_{zx}^{(12)}(x,x') \\
&= -L_2 g_{xz}^{(21)}(x,x') = L_2 g_{zx}^{(21)}(x,x') \\
&= 2\left(\operatorname{atan}\frac{d+L_1+L_2}{x-x'} - \operatorname{atan}\frac{d+L_1}{x-x'}\right. \\
&\quad \left. - \operatorname{atan}\frac{d+L_2}{x-x'} + \operatorname{atan}\frac{d}{x-x'}\right).
\end{aligned}
$$

The explicit expressions for all the other elements may be found in Ref. 11.

The introduction of additional coupling through nonidentical components of the dynamic magnetization accounts for the nonreciprocal nature of the Damon-Eschbach surface mode.[17] Each resonant mode in a magnetic trilayer is a superposition of four traveling waves, a pair of waves propagating in opposite directions in film 1, and a similar pair in film 2. In thin structures all the four waves are practically identical, thus forming two standing waves of equal amplitude in each film, that are either in phase (acoustical mode) or in antiphase (optical mode). In thicker structures, however, the waves traveling in the $+x$ direction have the tendency to be more pronounced in the top film 1, and those traveling in the $-x$ direction are more pronounced in the bottom film 2. This means that, apart from a standing wave pattern, there is a wave traveling in the $+x$ direction in the top film and in the $x$-direction in the bottom film. In other words, this propagating component circulates in the $xz$ plane in the direct counter clockwise direction, taking into account the positive direction of the $y$ axis.

Strictly speaking, similar redistribution of the dynamic magnetization takes place in each individual film. In this case, the diagonal approximation adopted in Ref. 11 is no longer valid and the theoretical description becomes far more complicated. In the context of this paper it is hardly justified from the practical point of view.

The developed code computing the resonance frequencies, as well as the mode profiles corresponding to each resonance, is extremely time-saving. It takes less than 10 s to calculate, on an up-to-date personal computer, the full set of frequencies and mode profiles, which makes it very useful for rapid and flexible analysis of experimental data.

## IV. EXPERIMENTAL RESULTS AND DISCUSSION

### A. Symmetric wires

Since we have restricted our research to the case of purely dipole interactions between two monolayers the investigated samples are relatively thick, the 10 nm thick copper spacer excluding any exchange coupling between the layers.

In Fig. 2 the experimental Brillouin light scattering spectra for both the continuous (unpatterned) trilayer and the symmetric NiFe(30 nm)/Cu(10 nm)/NiFe(30 nm) trilayered wires are shown. The NiFe/Cu/NiFe sandwich can be regarded as a system of two vertically coupled identical resonators. That is why, to the first approximation, the distribution along the vertical $z$ axis can be either quasi-symmetrical (acoustic modes) or quasi-anti-symmetrical (optic modes), denoted respectively $s1$, $s2$,… and $as1$, $as2$,…. As it was mentioned before, in the first case, the magnetizations in the two films are nearly identical and oscillate in phase, while in the second case they are in antiphase. Note that, strictly speaking, there is no absolute symmetry for the distributions because of the surface character of the Damon-Eshbach wave.

For the unpatterned sample, the acoustic and optic modes, associated with the in-phase and out-of-phase precession of the dynamic magnetizations in the two magnetic layers, are

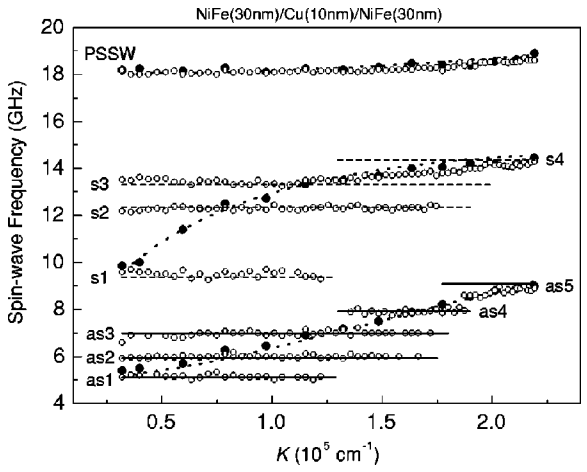


FIG. 3. Experimental (open points) and calculated spin-wave frequencies for the symmetric NiFe(30 nm)/Cu(10 nm)/NiFe(30 nm) trilayered wires as a function of the transferred in-plane wave vector $K$. Solid lines correspond to optical modes and dashed lines to acoustical ones. The external magnetic field $H=0.3$ kOe is applied along the $y$-axis, i.e., along the in-plane easy direction of the wires. For comparison the measured (full points) and calculated (dotted curves) frequencies of the unpatterned symmetric trilayer are also shown.

visible at 9.5 GHz and 5.5 GHz. In addition, the peak associated to the first perpendicular standing spin wave mode (PWWS) of a 30 nm monolayer is visible at 18 GHz. Instead, a number of discrete peaks corresponding to the quantization of the acoustic and optic modes are visible in the trilayered wires spectrum (lower panel of Fig. 2). The frequency dispersion of these modes as a function of the in-plane transferred wave vector is reported in Fig. 3. Note that all the modes are dispersionless, i.e. their frequency does not change as a function of the wavevector, and that the first bulk resonance mode is unaffected by patterning. The distance between adjacent wires being too great for the formation of collective modes, the phases of resonances on individual wires are not correlated, which means that the width of the spectral line in the $K$-space is of the order of $\pi/w$.[18]

From the fitting procedure to the experimental data of the unpatterned film we derive the magnetic parameter for the permalloy used in the calculation ($4\pi M_s=10.0$ kOe). The most striking feature seen in Fig. 2 are the resolved optical resonances. The explanation is straightforward. In the extreme case, of entirely separated films, i.e., $d\rightarrow\infty$, the two spectral branches are degenerate. When the spacer thickness $d$ becomes finite the degeneracy is removed due to dipolar coupling between the films. With the decrease of $d$ the dipolar coupling increases and the repulsion between the two branches becomes more and more pronounced. In the limit $d\rightarrow 0$ the optical branch tends to a horizontal line which means that the optical resonances do not depend on the resonance number, i.e. are degenerate. In our case, with the films separated by 10 nm, the system is far from the above mentioned limiting cases: the films are quite apart from each other, but the coupling is strong enough to separate the acoustical and the optical mode. Thus the degeneration in the optical mode is removed and the individual optical resonances are well resolved.

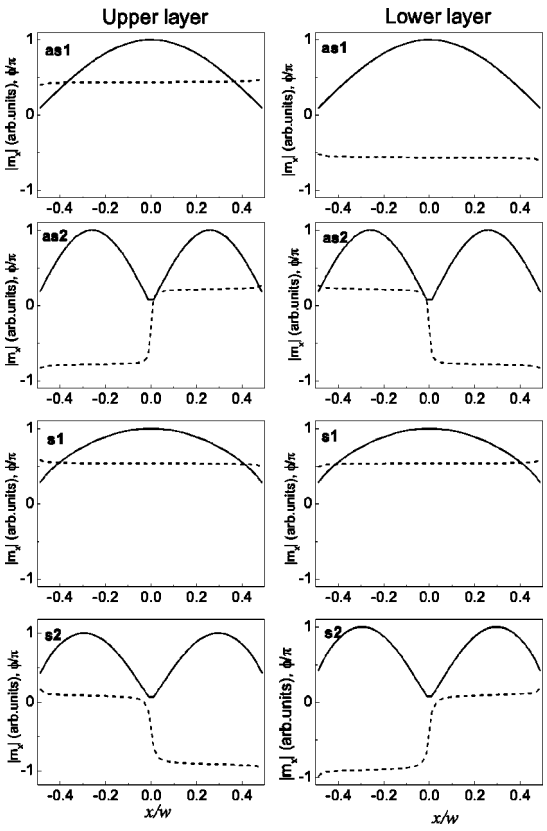


FIG. 4. Calculated amplitude of dynamic magnetization $|m_x|$ (continous curve) and its phase $\phi/\pi$ (dashed curves) for the lowest resonant modes in the symmetric NiFe(30 nm)/Cu(10 nm)/NiFe(30 nm) trilayered wires.

The theoretical predictions are in good, though not perfect, agreement with the experimental results. The difference between the two is of the same order of magnitude as the dispersion of the experimental points in an individual spectral line in the $K$-space. A somewhat more pronounced discrepancy is observed for the two higher optical resonances, which is not surprising. The improved technique reported in this paper extends its applicability up to $KL\approx 1$, which corresponds to the angle of incidence $\theta\approx 45°$. For higher values of $\theta$ the spatial frequency $K$ becomes so great that $KL>1$. In this case, as it was stated above, the diagonal approximation is no longer valid and additional terms of the Fourier expansion of the dynamic magnetization along "z" should be taken into account. Note that for thin structures, as those investigated in Ref. 12, our technique in its present form covers the whole range of $\theta$.

In Fig. 4 we present the calculated distributions of dynamic magnetization through the width of magnetic layers for the lowest two acoustic and optical resonances. Because of the diagonal approximation used in the calculation, any information on the thickness distribution of the dynamic magnetization is lost. The shown distributions can be regarded as those of the magnetization averaged through the layer thickness. Because the distributions are complex we show the absolute value of the amplitude of dynamic magnetization $|m_x|$ and its phase $\phi/\pi$. As stated above, because of the surface character of DE wave, a resonator in the form

of layered wire should have some similarity with an annular resonator, namely besides a standing wave a traveling wave should be present in each layer. The wave propagates in opposite directions in different layers. The calculated averaged distributions of magnetization show this tendency. They are complex with the phase which varies across the layer width. The variation of phase is nearly linear, of opposite signs in different layers, and much more pronounced for the higher-order resonances than for the lowest ones, which manifests the presence of traveling waves in the layers.

It is seen in Fig. 4 that the shape of the modal distribution is not exactly the same: while for antisymmetric modes (as1 and as2) it very close to the sinusoidal shape, it is not so for symmetrical modes (s1 and s2). In the latter case the curves are of more rounded shape and the effective width, at the 0.5 level, of the fundamental mode s1 is approximately 25% greater than that of as1. Another striking feature of the shown distributions first stated in Ref. 11 is a visible difference in the effective pinning conditions for different resonances. One sees that pinning for the antisymmetric mode is more pronounced, whereas for the both types of resonances it diminishes with the increase of the resonance number.

To explain this difference one has to consider the dipolar energy of the sample. Let us start with the homogenous precession in an in-plane magnetized unpatterned layered film. In the exchange-free case the frequency of both symmetric and antisymmetric modes of homogenous precession are equal. The only component of dynamic magnetization which gives rise to a dipolar field is the out-of plane component of the magnetization, $m_z$. Because the frequencies are equal, the dipolar energies associated with this component are equal for both the in-phase and the antiphase precession. Patterning of the film removes this frequency degeneracy, making the dipolar energies of the modes different. In particular, it influences the component of dynamic magnetization which is perpendicular to the "new" lateral surfaces, namely $m_x$. Thus to understand the physics of the redistribution of the dynamic magnetization in a patterned sample it suffices to consider the behavior of the component $m_x$.

To understand why the effective pinning of a symmetric mode is smaller than that of the antisymmetric with the same resonance number, one may consider how the force lines of the dynamic dipolar field can be closed in both cases. It is obvious that the orientation of $m_x$ in the opposite directions in different layers, which takes place in the lowest antisymmetric resonance, represents an energetically favorable situation, because in this case the force lines can be closed by directing them through the spacer and all the interlayer boundaries into the neighboring magnetic layer. As a result, the dipolar field near the lateral vertical surfaces decreases, therefore the magnetic moments near the edges are nearly not involved in the collective precession motion, which means their large effective pinning. The case of the symmetric modes is less favorable, because the force lines can only be closed by directing them into the same layer. Therefore a large scattered field is produced outside the magnetic layers. It results in a larger density of force lines leaving layers though their lateral surfaces. This result can be easily obtained while considering a symmetric structure with a vanishing spacer thickness, i.e., a monolayer. The higher density of force lines results in a larger effective magnetic charge on the lateral surfaces and, consequently, in the larger value of dynamic magnetization at the surface.

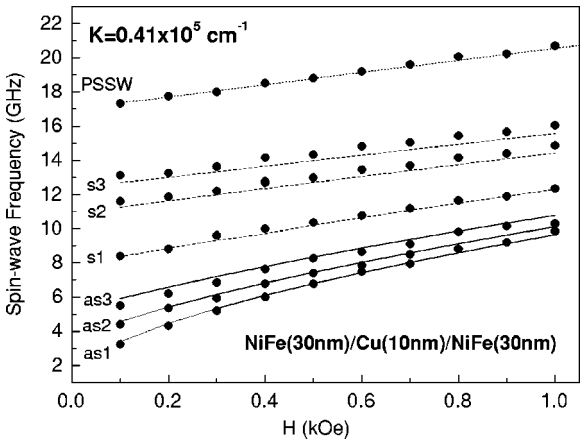


FIG. 5. Magnetic field dependence of the spin-wave modes frequency for the symmetric NiFe(30 nm)/Cu(10 nm)/NiFe(30 nm) trilayered wires. The geometry of the experiment is the same as in Fig. 2.

For the higher-order resonances, both symmetric and antisymmetric, the conditions of dynamic demagnetization for the same component $m_x$ are less favorable than for the lowest one, because in the same layer neighboring regions with a dynamic magnetization of opposite direction are now present. That "deforms" the field scattered outside the layers toward an increase of its density near the edges. It results in a higher charge density at the lateral surfaces, and, hence, in a smaller effective pinning there. Note for the symmetric resonances and the vanishing spacer thickness we recover the case of a single-layer wire considered in Ref. 9. There the same tendency of decrease of effective pinning with the resonance number was described.

To complete our analysis and to verify the interpretation of the modes character, the frequency dependence on the external field $H$ has been investigated. The measurements have been performed starting from 1.0 kOe and decreasing the field down to 0 kOe so that the wires are always in the saturated state. The comparison between the experimental points (filled circles) and the calculated frequencies (dotted line) is depicted in Fig. 5. Remarkably, the frequency of the symmetric modes is linear in $H$ while for the asymmetric ones there is small curvature in the low field range. As a comment to the overall behavior, one can note that the agreement between the measured and the calculated frequencies is rather good in the whole range of magnetic fields investigated. Since the angle of incidence was fixed at 10°, the theoretical analysis was carried out well within the limits of applicability of the method employed.

### B. Asymmetric wires

In Fig. 6, the experimental BLS spectra for the asymmetric unpatterned trilayer and the NiFe(30 nm)/Cu(10 nm)/NiFe(30 nm) trilayered wires are shown. These are measured in the same experimental conditions as those

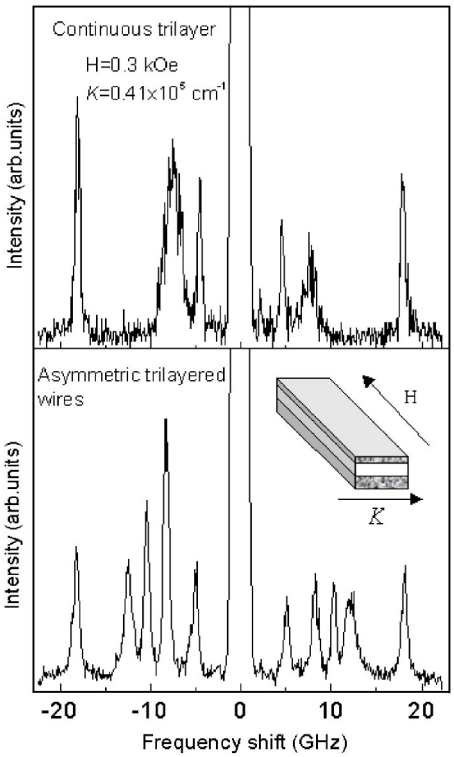


FIG. 6. BLS spectra for the asymmetric NiFe(10 nm)/Cu(10 nm)/NiFe(30 nm) trilayers: (upper panel) unpatterned trilayer and (lower panel) patterned trilayered wires. The spectra are taken in the same experimental conditions of Fig. 2.

reported in Fig. 2. The spectrum of the unpatterned trilayer is very similar to that of the continuous symmetric trilayer. Differences are visible instead in the BLS spectrum of the asymmetric trilayered wires. The spin wave frequency dispersion for the asymmetric structure together with the experimental frequencies for the unpatterned trilayer structure are summarized in Fig. 7.

Note that, contrary to the case of the symmetric trilayered wires, in this case the optic mode is not quantized and its frequency dispersion is almost equal to that of the unpatterned trilayer. Since the monolayers are not identical, the symmetry of the eigenmodes is broken. Consequently, the acoustical mode is not entirely symmetric, neither the optical one is entirely antisymmetric. For this reason the two modes are well separated even in the limit $d \to \infty$. In this case each mode is localized within one of the films. The slopes of the two branches, being proportional to the respective film thickness, are clearly different. When $d$ is finite the dipolar interaction has the tendency to further increase the separation between the branches, pushing the optical one towards a horizontal line. Since the two interacting modes, contrary to the case of a symmetric structure, are never in synchronism the repulsion is less pronounced. However, it is sufficiently strong to make individual resonances on the optical branch quasidegenerate and they are no longer resolved. That is why in Fig. 7 the theoretical results for the optical mode are presented in the form of a continuous dispersion curve. It connects the points (not shown in the figure) which correspond to resonance frequencies and corresponding effective

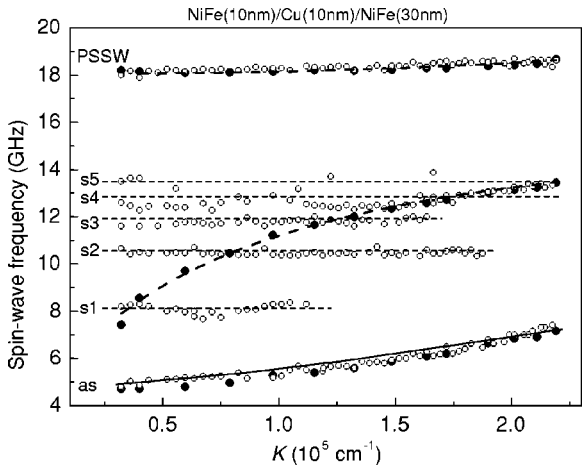


FIG. 7. Experimental (open points) and calculated spin-wave frequencies for the asymmetric NiFe(10 nm)/Cu(10 nm)/NiFe(30 nm) trilayered wires as a function of the transferred in-plane wave vector $K$. The external magnetic field $H=0.3$ kOe is applied along the $y$-axis, i.e., along the in-plane easy direction of the wires. For comparison the measured (full points) and calculated (dotted curves) frequencies of the unpatterned symmetric trilayer are also shown.

wave numbers, taking into account the "effective dipolar pinning"[9,11] at the edges of the stripe. A fairly good agreement between the theory and the experiment has been obtained, even if slight alterations in the value of the magnetomechanical ratio $\gamma$ were necessary to assure optimal fitting of the curves: $\gamma=2.856$ MHz/Oe in Fig. 3 and $\gamma=2.780$ MHz/Oe in Fig. 7.

Another striking feature of magnetic excitations in the non-symmetrical structures is the hybridization of modes.[11] The modal distributions on an asymmetric structure are presented in Fig. 8. In the particular case studied here, the acoustical modes are more prone to mixing than the optical ones. This can be explained in the following way. Any two oscillatory modes will interact only if the condition of phase synchronism is satisfied. More specifically, this means that the modes in question must have similar frequencies and wave numbers. Thus the selection rule is introduced. The width of a spectral line in the temporal frequency domain is relatively narrow. By contrast, due to the localization of the modes on a narrow stripe, it is very wide in the domain of the spatial frequencies $K$. In other words, while the values of resonance frequencies are well fixed, the corresponding peaks are markedly "smeared" in the $K$-space, which means that the selection rule is far more "strict" for the frequency than for the wave vector. That is why there is a strong hybridization of the acoustical mode s1 and the higher optical modes having neighboring frequencies. Similar hybridization between the mode s2 and the optical branch is less pronounced because the corresponding peaks overlap to a lesser degree in the $K$-space. As for the lower optical modes, their frequencies lie well below the lower boundary of the frequency band of the acoustic resonances. That is why no hybridization is possible and their modal profile is not perturbed in any way (e.g., see the profiles of as1 and as2 in Fig. 8).

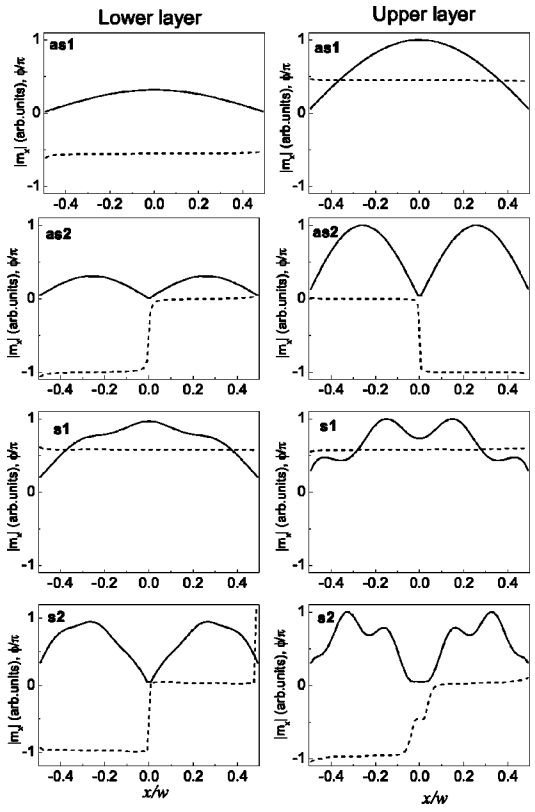


FIG. 8. Calculated amplitude of dynamic magnetization $|m_x|$ (continous curve) and its phase $\phi/\pi$ (dashed curves) for the lowest resonant modes in the asymmetric NiFe(10 nm)/Cu(10 nm)/NiFe(30 nm) trilayered wires.

Another noteworthy feature of the distributions shown in Fig. 8 is that, for the antisymmetric resonances, the amplitudes of dynamic magnetization are larger in thinner layers. The difference in amplitudes increases with the resonance number and for large resonance numbers the precession motion is mostly localized in the thinner layer. This phenomenon is also a manifestation of a worse phase synchronism of coupled resonances in the layers leading to a weaker coupling of them. As a result the antisymmetric mode is more localized in the thinner layer.

Finally, the frequency dependence on the intensity of the applied magnetic field for the asymmetric trilayered wires is reported in Fig. 9. Also in this case the agreement between calculated values and experimental frequency data is very good.

## V. CONCLUSION

The peculiarities of magnetostatic resonances on a trilayered (ferromagnetic/nonmagnetic spacer/ferromagnetic) wire with thick magnetic layers and thick spacer have been comprehensively studied, both theoretically and experimentally.

Experimentally Brillouin light scattering study of thermally excited spin waves has been performed as a function of the incidence angle of light and of the intensity of an external magnetic field applied along the wires axis. It was found that in a thick trilayer *symmetric* structure both acoustic (symmetric) and optical (antisymmetric) resonances can

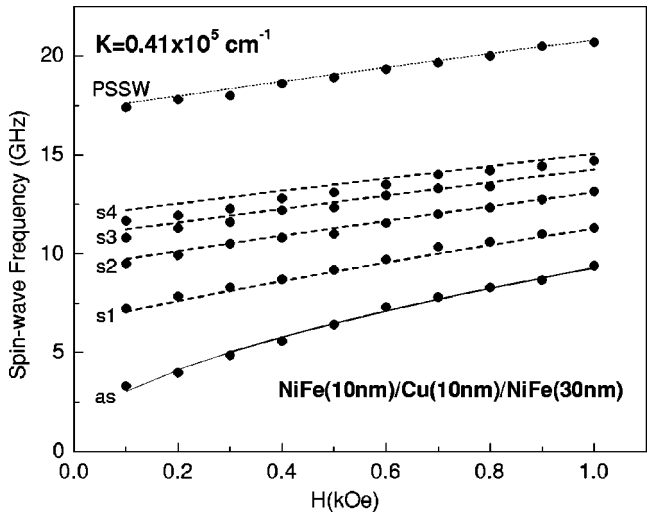


FIG. 9. Magnetic field dependence of the spin-wave resonant modes frequency for the asymmetric NiFe(10 nm)/Cu(10 nm)/NiFe(30 nm) trilayered wires.

be well-resolved. In the case of an *asymmetric* structure it was not possible to resolve the discrete spectrum of optical resonances and it appears as a continuous in-plane wave vector vs frequency dependence.

Theoretically it has been demonstrated that in this case the dipole interaction between magnetic layers associated with the nondiagonal terms of the tensorial Green functions $\hat{G}^{(21)}(x,x')$ and $\hat{G}^{(12)}(x,x')$ describing a dynamic dipolar magnetic field induced by one magnetic layer in the other one give significant contributions to the resonant frequencies. Besides, they make complex the eigendistributions of magnetization across the width of layers, which complicates their symmetry. The main feature of such complex distributions is the presence of a traveling wave besides a standing wave in each layer, which is a manifestation of the surface character of the Damon-Eschbach wave. However, in spite of the more complex symmetry compared to the previously investigated thin structure, in general outline the character of distributions remains the same, as well as the demagnetization conditions at the lateral surfaces of magnetic layers.

## ACKNOWLEDGMENTS

The work was supported in part by the French Ministry of National Education and Research (ACI NR0095 "NANODYNE"), by the Italian Ministry for the Instruction, University and Research (MIUR), by the Russian Foundation for Basic Research (Grant No. 02-02-16485), by the Russian Ministry of Education (Grant No. 1292) and by the Ministry of Education, Culture, Sports, Science and Technology of Japan through the Special Coordination Funds for Promoting Science and Technology (Nanospintronics Design and Realization, NDR). One of us (N.S.) also acknowledges her Co-Tutelle fellowship from French Ministry for Foreign Affairs, thereas M.K. acknowledges his Invited Professorship at the University Paris-13 and at the University of Perugia.

[1] N. Smith and P. Arnett, Appl. Phys. Lett. **78**, 1448 (2001).
[2] J. Shibata, K. Shigeto, and Y. Otani, Phys. Rev. B **67**, 224404 (2003).
[3] V. Novosad, M. Grimsditch, K. Yu. Guslienko, P. Vavassori, Y. Otani, and S. D. Bader, Phys. Rev. B **66**, 052407 (2002).
[4] V. Novosad, K. Yu. Guslienko, H. Shima, Y. Otani, S. G. Kim, K. Fukamichi, N. Kikuchi, O. Kitakami, and Y. Shimada, Phys. Rev. B **65**, 060402(R) (2002).
[5] R. Arias and D. L. Mills, Phys. Rev. B **67**, 094423 (2003).
[6] Z. K. Wang, M. H. Kuok, S. C. Ng, D. J. Lockwood, M. G. Cottam, K. Nielsch, R. B. Wehrspohn, and U. Gôsele, Phys. Rev. Lett. **89**, 027201 (2002).
[7] Y. Roussigné, S. M. Chérif, C. Dugautier, and P. Moch, Phys. Rev. B **63**, 134429 (2001).
[8] T. W. O'Keeffe and R. W. Patterson, J. Appl. Phys. **49**, 4886 (1978).
[9] K. Yu. Guslienko, S. O. Demokritov, B. Hillebrands, and A. N. Slavin, Phys. Rev. B **66**, 132402 (2002).
[10] M. P. Kostylev, A. A. Stashkevich, and N. A. Sergeeva, Phys. Rev. B **69**, 064408 (2004).
[11] M. P. Kostylev, A. A. Stashkevich, N. A. Sergeeva, and Y. Roussigné, J. Magn. Magn. Mater. **278**, 397 (2004).
[12] N. Sergeeva, S.-M. Chérif, A. Stachkevitch, M. Kostylev, and Y. Roussigné, Physica C **1**, 1587 (2004).
[13] V. D. Tsiantos, T. Schrefl, W. Scholz, and J. Fidler, J. Appl. Phys. **93**, 8576 (2003).
[14] *Spin Dynamics in Confined Magnetic Structures I and II*, edited by B. Hillebrands and K. Ounadjela (Springer, Berlin, 2003 and 2001).
[15] http://ghost.fisica.unipg.it/.
[16] J. R. Sandercock, in *Light Scattering in Solids III*, edited by M. Cardona and G. Güntherodt (Springer-Verlag, Berlin, 1982), p. 173.
[17] R. W. Damon and J. R. Eshbach, J. Phys. Chem. Solids **19**, 308 (1961).
[18] J. Jorzick, S. O. Demokritov, C. Mathieu, B. Hillebrands, B. Bartenlian, C. Chappert, F. Rousseaux, and A. Slavin, Phys. Rev. B **60**, 15194 (1999).